Absolute Organ Activity Estimated by Five Different Methods of Background Correction

Wilhelmina C.A.M. Buijs, Jeffry A. Siegel, Otto C. Boerman and Frans H.M. Corstens
University Hospital Nijmegen, Department of Nuclear Medicine, University of Nijmegen, The Netherlands

Accurate absorbed dose estimates in radionuclide therapy require patient-specific dosimetry. In patient-based dosimetry, estimation of absolute organ uptake is essential. The methods used should be reasonably accurate as well as easy to perform in routine clinical practice. One of the major sources of uncertainty in quantification of organ or tumor activity from planar images is the activity present in the tissue surrounding the source. **Methods:** To estimate organ activity as a function of organ-to-background activity concentration ratio, a cylindrical phantom, filled with 5.6 liters of water was used to simulate the abdomen of a patient. Two other cylinders of 150 ml each, representing the kidneys, were each filled with 19 MBq ^{99m}Tc and were positioned in the abdomen phantom. The phantom was imaged with a dual-head gamma camera with the kidneys placed at posterior depths of 1-, 5- and 10-cm at kidney-to-background activity concentration ratios of infinity, 10:1, 5:1 and 2:1. The conjugate view geometric mean counting method was used to quantify activity. Five methods for background correction were applied: (1) no correction; (2) conventional background correction (simple subtraction of the background counting rate from the source region counting rate); (3) Kojima method (background corrected for organ thickness and depth); (4) Thomas method (analytical solution); and (5) Buijs method (background corrected for organ and total-body thickness). **Results:** Since the results were identical for both kidneys, only the left kidney activity measurements are presented. The accuracy of the five background correction methods is given as the percentage difference between the actual and measured activity in the left kidney. For Method 1, the percentage difference ranged from −2% with an infinite kidney-to-background activity concentration ratio to +413% with a 2:1 ratio. For Method 2, these values ranged from −1% to −80%, for Method 3 from +11% to −18%, for Method 4 from −2% to +120% and for Method 5 from −4% to +39%. **Conclusion:** Even though quantitative SPECT is the most rigorous method for activity quantification in conditions of low organ-to-background activity concentration ratio, planar scintigraphy can be applied accurately if appropriate attention is paid to background correction. Using relatively simple background subtraction methods, the quantitative planar imaging technique can result in reasonably accurate activity estimates (Methods 3 and 5). The use of Kojima's method is preferable, especially at very low source-to-background activity concentration ratios.

Key Words: background correction; quantitative planar imaging; absolute organ activity

J Nucl Med 1998; 39:2167–2172

Estimation of absolute organ activity for the purpose of patient-based dosimetry in radionuclide therapy, particularly radioimmunotherapy, is of growing interest. The measurement of the biodistribution of radiopharmaceuticals and the use of these data in the Medical Internal Radiation Dose schema (*1,2*) provide the primary means to calculate absorbed doses from internally deposited radionuclides.

A series of physical factors contribute to the difference between measured activity and actual activity in source regions based on planar scintigraphy. Accurate estimation of the activity in an organ from the measured counting rate requires correction for the system calibration factor (measured counting rate per MBq), attenuation, scatter, background activity, organ- and patient thickness and physical decay of the radionuclide used. Because activity in surrounding organs and nonuniform distribution of background may interfere with accurate quantification, SPECT imaging has the potential to improve the accuracy of planar imaging measurements (*3–7*). However, because of the time-consuming and more complex nature of quantifying SPECT image data, there is a need for a reasonably accurate and simple quantification method based on planar imaging.

Several techniques for activity quantification of planar images have been studied, most of them dealing with attenuation and other corrections using the conjugate view counting method (*8–18*). In situations with low target-to-background activity concentration ratios, such as in radioimmunotargeting, accurate background correction is very important. Different methods of background correction have been described (*9,19–20*).

In this study, the accuracy of five different methods for background correction is compared at various organ-to-background activity concentration ratios.

MATERIALS AND METHODS

Phantom

A cylindrical phantom with an inner diameter of 21.5 cm was filled with 5.6 liters of water to simulate the abdomen of a patient (Fig. 1). The thickness of the acrylate (density: 1.18 g/cm^3) cylinder wall was 0.3 cm. The length of the large cylinder (H) was 18 cm (Fig. 1B). Two other cylinders with an inner diameter of 5.2 and an outer diameter of 5.5 cm (t_m), representing the kidneys, were each filled with a solution of 19 MBq ^{99m}Tc-pertechnetate in 150 ml water (Fig. 1A). The height of the water-level in the small phantoms was 7 cm (h; Fig. 1B). The thickness of the part of the large cylindrical phantom that included the kidney cylinders (T) was 18.5 cm (Fig. 1A). The kidneys were positioned in the abdomen phantom at three different depths (d). The distances between the posterior kidney surface and the posterior abdominal cylinder wall in these three positions were approximately 1, 5 and 10 cm (Fig. 1B). The axis between the centers of the two kidney cylinders was parallel to the detector, and the distance between the centers was 10.5 cm.

In some of the background correction methods described in this study, the thickness of the source, measured in the direction perpendicular to the gamma camera surface, must be known. Because the shape of the cross section in a cylindrical phantom is circular, the thickness would vary along the direction parallel to the gamma camera surface. To get a constant (virtual) thickness along the direction parallel to the gamma camera surface, an effective thickness was calculated (t). This effective thickness was defined as the height of a rectangle, which has a width equal to the diameter of the cylinder and an area equal to the area of the circular cross section of the small cylinder. The height of that rectangular is then: $\frac{1}{4}\ \pi\ t_m^2/t_m$, where t_m is the diameter of the small cylinders (5.5 cm). Thus, the effective thickness t is equal to 4.3 cm.

Received Oct. 1, 1997; revision accepted Mar. 24, 1998.
For correspondence or reprints contact: Wilhelmina C.A.M. Buijs, PhD, Department of Nuclear Medicine, University Hospital Nijmegen, 6500 HB Nijmegen, The Netherlands.

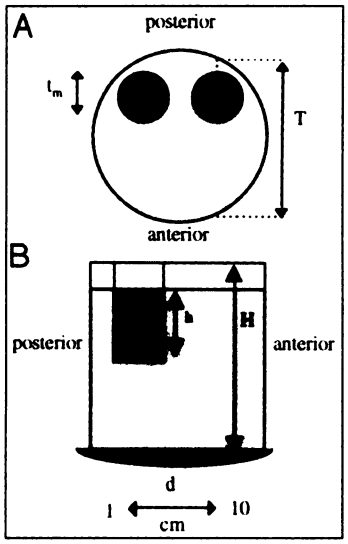

FIGURE 1. Top (A) and side (B) views of phantom with two kidney cylinders inserted in large abdomen cylinder. (A) T is thickness of part of large cylindrical phantom that includes kidney cylinders (18.5 cm), and t_m is diameter of small cylinder (5.5 cm). (B) H is length of large cylinder (18 cm), h is height of activity-solution in small kidney cylinders (7 cm) and d is depth of kidney phantoms (1, 5 and 10 cm from posterior wall of large cylinder). Large cylinder was not filled to top of cylinder to make it possible to stir solution in cylinder after each new addition of activity to reach uniform distribution of activity in background compartment.

Various kidney-to-background activity concentration ratios were obtained by adding ^{99m}Tc-pertechnetate to the background (abdomen cylinder), while keeping the activity in the kidneys constant. Kidney-to-background activity concentration ratios of infinity (no background activity) and approximately 10:1, 5:1 and 2:1 were achieved. After the activity was uniformly distributed in the various compartments, a sample of 2 ml was taken from each kidney phantom at the start of the study; 2-ml samples were also taken from the solution in the large cylinder for each of the kidney-to-background activity concentration ratios. The purpose of taking the initial 2-ml sample from the abdominal phantom (when no background activity was present) was to ensure that the kidney cylinders were not leaking activity. At the end of the imaging study, 0.5 ml aliquots from each 2-ml-kidney and 2-ml-background sample were measured in a well-counter and activity concentration in cpm/g was calculated. Exact kidney-to-background activity concentration ratios were determined by comparing the activity concentration in the samples taken from the kidney cylinders with the activity concentration in the samples taken from the abdominal phantom for the four different background situations.

Imaging

The phantom was imaged with a dual-head gamma camera (MultiSPECT 2; Siemens, Hoffman Estates, IL) equipped with parallel-hole, low-energy, high-resolution collimators connected to a computer (ICON; Siemens). A symmetric 15% window was set at 140 keV. The phantom was placed upright on the scanning table, and the detectors were placed in vertical positions 180° opposed to each other. For each of the four kidney-to-background activity concentration ratios, the kidneys were moved from the 1-cm to 5-cm to 10-cm depths. Anterior and posterior static images were acquired during 5 min and stored in a 256 × 256 matrix. For each of the two detectors, the system calibration factor for ^{99m}Tc was determined in counts per minute (cpm)/MBq.

Analysis and Background Correction

On the posterior image with no background activity in the large cylinder, a rectangular region of interst (ROI) (28 × 36 pixels) was drawn manually around the left kidney, which was positioned at a depth of 1 cm from the background surface of the large cylinder. The same ROI was positioned on the right kidney and on the background area beneath the left kidney. These ROIs were then superimposed on the images with background activity (Fig. 2). The measured ROI counting rates (cpm) were corrected for physical decay.

To quantify the activity in the kidney cylinders, the conjugate view counting method was used (*9*):

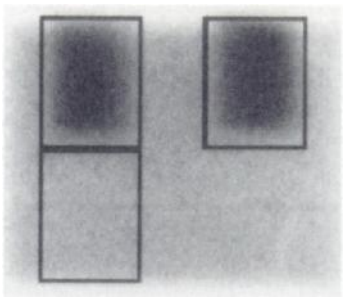

FIGURE 2. Posterior image of phantom at kidney-to-background activity concentration ratio of 10:1. Kidney cylinders are positioned at depth of 5 cm from posterior wall of large cylinder. Rectangular ROIs used for kidneys and background are shown.

$$A = \left(\frac{I_A I_P}{e^{-\mu_e T}}\right)^{1/2} \frac{f}{C}, \qquad \text{Eq. 1}$$

where A is the kidney activity in MBq, I_A and I_P are the anterior and posterior view counting rates, respectively (cpm), T (cm) is the thickness of the abdominal cylinder at the position of the kidney cylinders (18.5 cm), μ_e (cm^{-1}), is the effective total linear attenuation coefficient (for the abdomen phantom an experimentally derived effective attenuation coefficient for ^{99m}Tc of 0.143 cm^{-1} was used), f is equal to $(\mu_e t/2)/\sinh(\mu_e t/2)$ and represents a correction for the source region attenuation coefficient (μ_e) and source thickness (t) (i.e., source self-attenuation correction); it was determined to be 0.98 and C is the system calibration factor (counting rate per unit activity). The system calibration factor used in this study (5540 cpm/MBq) was obtained by counting a known activity of ^{99m}Tc for a fixed period of time in air using the same camera, collimators and camera acquisition settings as for the phantom study.

The effective linear attenuation coefficient was determined using a transmission phantom consisting of a series of acrylic plates (tissue-equivalent material) each with a diameter of 42 cm and a thickness of 2–3 cm (density 1.18 g/cm^3). A hollow circular phantom 8.5 cm in diameter was filled with a solution of 30 MBq ^{99m}Tc to a height of 2.5 mm. Images of 5 min were acquired for the source in air and then with consecutive thicknesses of tissue-equivalent material in steps of 2 cm up to 23.6 cm. Transmission factors were measured using an ROI size equal to the size of the ROIs in the kidney phantom study. Curve fitting the resulting transmission factor versus depth curve resulted in an attenuation coefficient of 0.143 cm^{-1} (μ_e) and a buildup factor of 1.07 (*21*). For small ROI sizes, the buildup factor is small and was not used in our analysis.

The following five methods of background correction were applied to estimate the absolute kidney activity:

1. No background correction: Equation 1 is applied with measured I_A and I_P without correction for background activity.
2. Conventional background subtraction: The counting rate measured in an adjacent ROI was subtracted from the counting rate in the kidney ROI, according to:

$$I_A = I'_A - I_{BGA}, \quad \text{and}$$

$$I_P = I'_P - I_{BGP}, \qquad \text{Eq. 2}$$

where I_A (I_P) is the background corrected counting rate in the anterior (posterior) kidney ROI, I'_A (I'_P) is the measured counting rate in the anterior (posterior) kidney ROI and I_{BGA} (I_{BGP}) is the counting rate in the anterior (posterior) background ROI. These I_A (I_P) counting rates are used in Equation 1. The activity in the background ROI was expressed as cpm per pixel. This counting rate was multiplied by the number of pixels in the kidney ROI and then subtracted from the total counts in the kidney ROI.

3. Kojima Method: This method corrects for over-subtraction of background activity by taking into account the size of the

TABLE 1
Total Counts in Five-Minute Images

Activity concentration ratio	Posterior depth (cm)	Anterior image	Posterior image
Infinity	1	199816	656483
	5	303157	400016
	10	553473	224559
10:1	1	991048	1301297
	5	1033779	1057713
	10	1217281	898773
5:1	1	1633057	1816363
	5	1669148	1631166
	10	1788251	1463417
2:1	1	3342533	3275677
	5	3320268	3120964
	10	3331846	2984341

kidney and assuming a uniform background activity concentration (*19*):

$$I_A = I'_A - I_{BGA} \times C_A, \quad \text{and}$$

$$I_P = I'_P - I_{BGP} \times C_P, \qquad \text{Eq. 3}$$

where C_A (C_P) is the multiplication factor for the anterior (posterior) background counting rate, defined as:

$$C_A = 1 - \frac{e^{-\mu_0(T-d-t)} \cdot [1 - e^{-\mu_0 t}]}{1 - e^{-\mu_0 T}}, \quad \text{and}$$

$$C_P = 1 - \frac{e^{-\mu_0 d} \cdot [1 - e^{-\mu_0 t}]}{1 - e^{-\mu_0 T}}. \qquad \text{Eq. 4}$$

The second term in each of these equations is the correction for the background counting rate equivalent to the volume of the kidney at depth d from the background surface to the posterior aspect of the kidney, t is the effective thickness of the kidney, T is the thickness of the abdomen phantom and μ_0 is the narrow beam linear attenuation coefficient (equal to 0.15 cm^{-1} for ^{99m}Tc). The correction factors C_A and C_P were calculated using a BASIC program with the appropriate values of d (i.e., 1, 5 and 10 cm), t (effective) = 4.3 cm and T = 18.5 cm. These I_A (I_P) counting rates determined from Equations 3 and 4 are used in Equation 1.

4. Thomas Method: Quantification using the conjugate view counting method in combination with an analytical method for background correction was applied (*9*):

$$A = \left(\frac{I_A I_P}{e^{-\mu_0 T}}\right)^{1/2} \frac{f}{C} \times k(\gamma). \qquad \text{Eq. 5}$$

Equation 1 was multiplied by $k(\gamma)$, where $k(\gamma)$ is the background correction factor defined as:

$$k(\gamma) = \{1 + (\gamma_2 f_3/f_2)^2 + (\gamma_4 f_3/f_4)^2 + 2\gamma_2\gamma_4(f_3^2/f_2 f_4) \cosh[(\mu_2 t_2 + 2\mu_3 t_3 + \mu_4 t_4)/2] + 2\gamma_2 f_3/f_2 \cosh[(\mu_2 t_2 + \mu_3 t_3)/2] + 2\gamma_4 f_3/f_4 \cosh[(\mu_3 t_3 + \mu_4 t_4)/2]\}^{-1/2}. \qquad \text{Eq. 6}$$

The subscripts 2, 3 and 4 represent the anterior background region, kidney region and posterior background region, respectively. The individual f-factors are as previously defined according to $(\mu_j t_j/2)/\sinh(\mu_j t_j/2)$, while $\gamma_2 \equiv A_2/A_3$ and $\gamma_4 \equiv A_4/A_3$ represent the ratios of the activity in the adjacent regions to that in the source volume.

The value of the factor $k(\gamma)$ thus depends on the organ-to-background activity concentration ratio, thickness of the source organ, thicknesses of the background volumes anterior and posterior to the kidneys and the attenuation coefficients for tissue layers with different densities. The $k(\gamma)$ factors were calculated for all three positions of the kidney in the abdomen phantom, thus for three pairs of background thicknesses and for the four kidney-to-background activity concentration ratios (infinity, 10:1, 5:1 and 2:1) using a software program written in BASIC.

5. Buijs Method: A simple, geometrically based subtraction technique was applied to correct for over-subtraction of background activity, as a consequence of the volume occupied by the organ (*20*):

$$I_A = I'_A - I_{BGA} \times F, \quad \text{and} \qquad \text{Eq. 7}$$

$$I_P = I'_P - I_{BGP} \times F,$$

where I_A, I'_A, I_{BGA} and I_P, I'_P and I_{BGP} are the same as in Equation 2. F is the fraction of the total background activity I_{BGA} to be subtracted from the measured activity in the source organ ROI, I'_A (I'_P) and is defined as:

$$F = 1 - (t/T), \qquad \text{Eq. 8}$$

where t is the thickness of the source organ and T is the thickness of the abdomen cylinder through the source ROI. In this study, t is the effective diameter of the kidney (4.3 cm) and T is 18.5 cm. Therefore, F was calculated to be 0.76 (1- [4.3/18.5]). The I_A (I_P) counting rates determined from Equations 7 and 8 are used in Equation 1.

RESULTS

Because the results for both kidney cylinders were virtually identical, only results for the left kidney are presented here. The measured activity in the left kidney at the start of the phantom study was 19.3 MBq ^{99m}Tc. The actual activity concentration ratios between the left kidney and the background (abdominal volume) were 10.1:1, 5.01:1 and 2.15:1, respectively. The total counts per 5-min image are presented in Table 1. The maximum counting rate found during the measurements was 11.3 kcps; therefore, dead time did not play a role.

The exact depths of the kidneys and the related background correction factors for the Kojima method are presented in Table 2. The correction factors were calculated using Equation 4.

The Thomas $k(\gamma)$ background correction factors were calculated for the three different kidney depths and for the four kidney-to-background activity concentration ratios (Table 3).

TABLE 2
Background Correction Factors at Different Depths (Kojima Method)

Distance between kidney and posterior abdomen (cm)	Kidney anterior depth (cm)	Kidney posterior depth (cm)	Background correction factor (anterior) C_A	Background correction factor (posterior) C_P
1	12.6	1.6	0.92	0.61
5	8.6	5.6	0.86	0.78
10	3.6	10.6	0.71	0.89

TABLE 3
k(γ) for Background Correction (Thomas Method)

Kidney-to-background activity concentration ratio posterior depth (cm)	Infinity	10:1	5:1	2:1
1	1	0.76	0.63	0.42
5	1	0.78	0.64	0.44
10	1	0.77	0.63	0.43

The relation between estimated activity in the left kidney and the kidney-to-background activity concentration ratio was different for the five methods of background correction (Fig. 3). When no background activity was present, the difference between the estimated activity in the left kidney and the actual activity for all five background correction methods at all three positions of the kidney cylinders ranged from −4 to +1% (Table 4). If no background correction was applied, overestimation from 77% for the kidney-to-background activity concentration ratio of 10:1, up to 413% in the case of the lowest kidney-to-background activity concentration ratio of 2:1 was found (Table 4). Conventional background subtraction resulted in an underestimation of the actual activity, ranging from −22% to −80% with decreasing kidney-to-background activity concentration ratios. For the Kojima method, the differences in estimated activity and actual activity varied from −18% to +11%. Using the Thomas method, the activity was overestimated, gradually increasing with decreasing kidney-to-background activity concentration ratios, to a difference of 120% between the estimated activity and the actual activity at the 2:1 ratio. For the Buijs method, the differences in estimated activity and actual activity ranged from +2% to +39%. The overall differences between kidney activity estimated from the phantom measurements and the actual activity in the kidney ranged from −80% to +413% (Table 4).

DISCUSSION

Biodistribution data for radiopharmaceuticals within the body and specific organs may be obtained from planar scintillation camera views using the conjugate view geometric mean technique. The accuracy of this method will be greatest for radiopharmaceuticals distributed in a single organ or isolated organs that do not overlap in the planar projection. However, in most nuclear medicine examinations, background activity will be present in adjacent tissues. For planar gamma camera imaging, subtraction of background activity present in surrounding tissue from activity measured in the organ of interest is routinely performed. Background subtraction is required to allow accurate estimation of the organ activity or for comparisons of relative activity uptakes or retentions between tissues. The adequacy of background subtraction is especially important for the accurate estimation of the activity in the red marrow (*22,23*), since red marrow is the dose-limiting toxicity in most, if not all, radionuclide therapy and radioimmunotherapy.

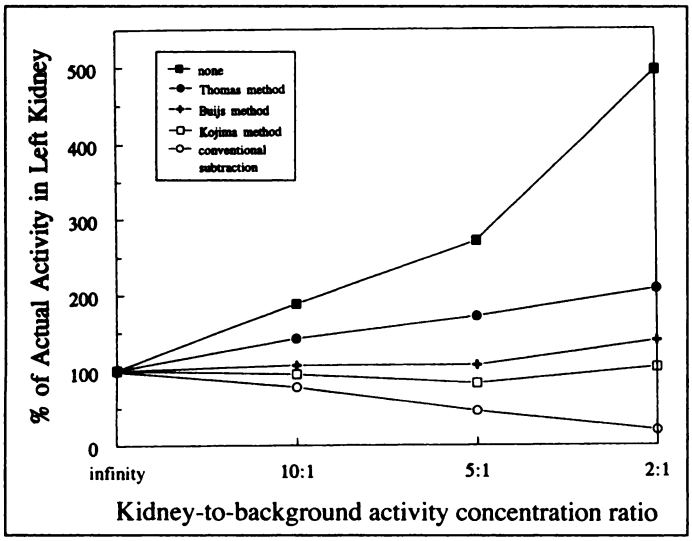

FIGURE 3. Percent of actual activity in left kidney at depth of 1 cm from background surface to posterior aspect of kidney, as function of kidney-to-background activity concentration ratio, for all five methods of background correction.

This phantom study was performed to determine the optimal method of background correction. The accuracy of the absolute activity determination in the kidney phantom was evaluated using five different methods of background correction and planar imaging, for three different organ depths and four organ-to-background activity concentration ratios: infinity (meaning no activity in the background at all), 10:1, 5:1 and 2:1. Two kidney inserts were used to simulate the clinical situation where cross scatter between activity in the kidneys may occur. The results were virtually identical for both kidneys; therefore, only the results for the left kidney were presented.

As all images were uniformly acquired for 5 min each, the counting statistics will differ between the images at different source-to-background activity concentration ratios (achieved by adding different amounts of activity to the abdominal phantom). This may somewhat affect the results due to the statistical uncertainties (i.e., noise) in the resulting images. However, if fixed counts per image would have been acquired, the results could also be affected since most of the counts will come from the background as the background activity is raised and the image acquisition time is shortened. As the acquisition time is shortened for the same number of counts, the statistical uncertainty in the counting rate (defined as the square root of the number of counts divided by the acquisition time) will increase. So, irrespective of the methods used to acquire the data, some statistical uncertainty would result.

Application of the conjugate-view method to actual patients generally involves some sort of transmission imaging for estimation of the attenuation term. In this phantom-study, the attenuation coefficient (μ_e) was estimated by transmission measurements in a tissue-equivalent phantom using the same camera, collimators and camera acquisition parameters as in the kidney-phantom study.

In the absence of background activity, the difference between the estimated activity in the left kidney and the actual activity for all five background correction methods at all three positions of the kidney cylinders, was highly accurate and ranged from −4% to +1% (Table 4). These results indicate that the method of attenuation correction applied in this study is reliable and yields accurate results in a zero-background situation.

Obviously, in the presence of background activity, background correction must be performed (Table 4). The most common method used for background correction is to subtract the counts in a selected background ROI from the counts in the ROI drawn over the organ of interest (representing the sum of activity in the organ and in the surrounding background). Such a conventional background correction method leads inevitably to an over-correction since the volume of the organ of interest is not considered, thus leading to a large underestimation of the true activity in the organ. In our phantom model, the underestimation rose with increasing background activity from 22% to 80%.

TABLE 4
Percentage Difference Between Estimated and Actual Activity in Left Kidney

Activity concentration ratio	Posterior depth (cm)	No background correction	Conventional background correction	Kojima method	Thomas method	Buijs method
Infinity	1	1	−1	−1	1	0
	5	−2	−4	−4	−2	−4
	10	−1	−3	−2	−1	−2
10:1	1	88	−22	−5	42	7
	5	77	−22	−4	38	2
	10	81	−24	−6	40	2
5:1	1	171	−54	−17	71	7
	5	168	−35	2	71	14
	10	166	−56	−18	68	3
2:1	1	396	−80	4	108	39
	5	400	−75	11	118	39
	10	413	nd	−11	120	32

nd = not determined.

The no-background-correction method and the conventional method for background correction do not correct for source volume, in contrast to the Kojima, Thomas and Buijs methods.

Kojima's background correction method corrects for source volume (*19*) and was originally used with the depth-independent buildup factor method (DIBF) for attenuation correction (*19,21,24,25*). However, in this study, the geometric mean method (Eq. 1) was used for attenuation correction, instead of the DIBF method, in combination with Kojima's background correction method for estimating the organ activity. This modified Kojima method is easy to perform and provides reliable results if organ thickness, derived from CT images or from anatomical atlas data, are available and patients' thickness is measured as well (Table 4; Fig. 3). Recently, Kojima et al. (*26*) refined their method for quantitative planar imaging using a combination of a transmission image and a conjugate view emission image. The triple-energy window method for scatter correction of the emission and transmission images was used. Applying this method to their kidney phantom, they found differences of less than 5% between the estimated and actual activity for source-to-background activity concentration ratios from 40:1–5:1. These results are better than the results of our study using their earlier described method (*19*), where differences of 5% and 17% for source-to-background activity concentration ratios of 10:1 and 5:1, respectively, were found.

Thomas' method does not use a background subtraction technique but introduces a multiplication factor $k(\gamma)$ for background correction, in combination with Equation 1. The results of Thomas' method were not very accurate, with a maximum difference of 120% between estimated and actual activity in the kidney at a kidney-to-background activity concentration ratio of 2:1. This may be explained by the fact that this method does not correct for scatter, since the formula for $k(\gamma)$ was derived under the condition of narrow-beam geometry. The method may, therefore, be inadequate for low organ-to-background activity concentration ratios, since as the background activity is increased, more scatter radiation will be present in the source ROI. This analytical method is not based on the measurement of actual background activity, but needs a priori global knowledge of the source-to-background activity concentration ratio. This may be a disadvantage.

The Buijs method also requires a correction factor for the source volume. This factor is simply the ratio between the source thickness and the patient thickness (*27*). To use this method for quantitative organ uptake in clinical practice, a one-time estimation of the broad beam (effective) attenuation coefficient (μ_e, cm^{-1}) must be calculated from phantom-based transmission curve measurements, for each combination of radionuclide, window settings, collimator and camera.

For all five methods of background correction, the differences between estimated and actual activity in the kidney varied only slightly with source depth.

At low kidney-to-background activity concentration ratios (2:1), Kojima's method is more accurate than Buijs' method. However, both methods yield results of estimated activity that are reasonably accurate and reliable for use in routine clinical practice.

Finally, it must be stated that the results of any phantom-based study represent a best-case scenario. Phantom-based studies of radionuclide quantitation, including the current study, generally have limitations, including the inability to accurately simulate the irregularity and nonuniformity of background activities and the irregular sizes, shapes, compositions and, therefore, linear attenuation coefficients of source and nonsource regions. In patient studies, less accurate activity estimations may result due to variations in background activity concentrations, the size of the ROIs used in the data analysis, variations in and inaccurate estimates of body thickness, organ thicknesses and organ depths.

CONCLUSION

This phantom study shows that the use of the Kojima or Buijs methods for background correction, combined with quantitative planar imaging, provides more accurate results for the estimation of actual activity in an organ, compared with methods without background subtraction or with conventional background correction. The use of Kojima's method is preferable, especially at very low source-to-background activity concentration ratios.

ACKNOWLEDGMENT

We thank Mr. A. Meeuwis for technical assistance.

REFERENCES

1. Loevinger R, Berman M. A revised schema for calculating the absorbed dose from biologically distributed radionuclides. *MIRD pamphlet no. 1, revised.* New York: Society of Nuclear Medicine; 1976.
2. Loevinger R, Budinger TF, Watson, EE. *MIRD primer for absorbed dose calculations, (rev. ed.).* New York: Society of Nuclear Medicine; 1991.
3. Rosenthal MS, Cullom J, Hawkins W, Moore SC, Tsui BMW, Yester M. Quantitative SPECT imaging. A review and recommendations by the focus committee of the Society of Nuclear Medicine Computer and Instrumentation Council. *J Nucl Med* 1995;36:1489–1513.

4. Zanzonico PB, Bigler RE, Sours G, Strauss A. Quantitative SPECT in radiation dosimetry. *Semin Nucl Med* 1989;19:47–61.
5. Tsui BMW, Zhao X, Frey EC, McCartney WH. Quantitative single-photon computed tomography. Basics and clinical considerations. *Semin Nucl Med* 1994;24:38–65.
6. Tsui BMW, Frey EC, Zhao X, Lalush DS, Johnson RE, McCartney WH. The importance and implementation of accurate 3D compensation methods for quantitative SPECT. *Phys Med Biol* 1994;39:509–530.
7. Parker JA. Quantitative SPECT: basic theoretical considerations. *Semin Nucl Med* 1989;19:3–12.
8. Graham LS, Neil BA. In vivo quantitation of radioactivity in using the Anger camera. *Radiology* 1974;112:441–442.
9. Thomas SR, Maxon HR, Kereiakes JG. In vivo quantitation of lsion radioactivity using external counting methods. *Med Phys* 1976;3:253–255.
10. Sorenson JA. Methods for quantitating radioactivity in vivo by external counting measurements [PhD thesis]. Madison, WI: University of Wisconsin; 1971.
11. Fleming JS. A technique for the absolute measurement of activity using a gamma camera and computer. *Phys Med Biol* 1979;24:176–180.
12. Reenen O van, Lötter MG, Heyns A du P, et al. Quantification of the distribution of ^{111}In-labeled platelets in organs. *Eur J Nucl Med* 1982;7:80–84.
13. Macey DJ, Marshall R. Absolute quantitation of radiotracer uptake in the lungs using a gamma camera. *J Nucl Med* 1982;23:731–734.
14. Eary JF, Appelbaum FL, Durack L, Braun P. Preliminary validation of the opposing view method for quantitative gamma camera imaging. *Med Phys* 1989;16:382–387.
15. Gainey MA, Siegel JA, Smergel M, Jara BJ. Indium-111-labeled white blood cells: dosimetry in children. *J Nucl Med* 1988;29:689–694.
16. Rensburg AJ, Lötter MG, Heyns AP, Minnaar PC. An evaluation of four methods of ^{111}In planar image quantification. *Med Phys* 1988;15:853–861.
17. Hammond N, Moldofsky P, Beardsley M, Mulhern C Jr. External imaging techniques for quantitation of distribution of ^{131}I F(ab')2 fragments of monoclonal antibody in humans. *Med Phys* 1984;11:778–783.
18. Ott RJ. Imaging technologies for radionuclide dosimetry. *Phys Med Biol* 1996;41: 1885–1894.
19. Kojima M, Takaki Y, Matsumoto M, et al. A preliminary phantom study on a proposed model for quantification of renal planar scintigraphy. *Med Phys* 1993;20:33–37.
20. Buijs WCAM, Massuger L, Claessens RAMJ, Kenemans P, Corstens FH. Dosimetric evaluation of immunoscintigraphy using indium-111-labeled monoclonal antibody fragments in patients with ovarian cancer. *J Nucl Med* 1992;33:1113–1120.
21. Wu RK, Siegel JA. Absolute quantitation of radioactivity using the buildup factor. *Med Phys* 1984;11:189–192.
22. Siegel JA, Lee RE, Pawlyk DA, Horowitz JA, Sharkey RM, Goldenberg DM. Sacral scintigraphy for bone marrow dosimetry in radioimmunotherapy. *Nucl Med Biol* 1989;16:553–559.
23. Siegel JA, Wessels BW, Watson EE, et al. Bone marrow dosimetry and toxicity for radioimmunotherapy. *Antibody Immunuconj Radiopharm* 1990;3:213–233.
24. Siegel JA, Wu RK, Maurer AH. The buildup factor: effect of scatter on absolute volume deermination. *J Nucl Med* 1985;26:390–394.
25. Siegel JA. The effect of source size on the buildup factor calculation of absolute volume. *J Nucl Med* 1985;26:1319–1322.
26. Kojima A, Ohyama Y, Tomiguchi S, Kira M, Matsumoto M, Takahasi M. Quantitative planar imaging method for measuring renal activity using a conjugate-emission image and transmission data [Abstract]. *J Nucl Med* 1997;38:208P.
27. Buijs WCAM, Siegel JA, Corstens FHM. Estimation of absolute organ activity using five different methods of background correction: a phantom study [Abstract]. *Eur J Nucl Med* 1997;24:931.

Technetium-99m-Labeled Liposomes to Image Experimental Colitis in Rabbits: Comparison with Technetium-99m-HMPAO-Granulocytes and Technetium-99m-HYNIC-IgG

Els Th.M. Dams, Wim J.G. Oyen, Otto C. Boerman, Gert Storm, Peter Laverman, Emile B. Koenders, Jos W.M. van der Meer and Frans H.M. Corstens

Departments of Nuclear Medicine and Internal Medicine, University Hospital Nijmegen; and Utrecht Institute for Pharmaceutical Sciences, Department of Pharmaceutics, Utrecht University, The Netherlands

Scintigraphic techniques are routinely used for the evaluation of the extent and severity of inflammatory bowel disease. Currently, the radiopharmaceutical of choice is ^{99m}Tc-hexamethyl propyleneamine oxime (HMPAO)-leukocytes. We studied the imaging potential of two recently developed ^{99m}Tc-labeled agents, polyethylene glycol (PEG)-coated liposomes and hydrazinonicotinate (HYNIC) IgG, in a rabbit model of acute colitis, and compared them with that of ^{99m}Tc-labeled, granulocyte-enriched (>90%), white blood cells. **Methods:** Acute colitis was induced in rabbits by retrograde instillation of trinitrobenzene sulfonic acid. After 48 hr, 37 MBq of each radiopharmaceutical was administered intravenously. Gamma camera images were taken at 0, 1, 2, 4, 10 and 24 hr. At 4 and 24 hr postinjection, groups of rabbits were killed, and the uptake of the radiolabel in the dissected tissues was determined. For each affected 5-cm segment, the colitis index (CI, affected-to-normal-colon-uptake ratio) was calculated and correlated to the macroscopically scored severity of inflammation. **Results:** All three agents visualized the colitis lesions within 1 hr postinjection. The CI correlated with the severity of the abnormalities. With increasing severity, the CI at 4 hr postinjection for liposomes was 3.89 ± 0.73, 4.41 ± 0.47 and 5.76 ± 0.65; for IgG 1.67 ± 0.08, 3.92 ± 0.44 and 6.14 ± 0.65; and for granulocytes 2.90 ± 0.09, 6.15 ± 0.96 and 9.36 ± 3.35. For liposomes, the CI further increased during 24-hr postinjection to 6.56 ± 0.84, 8.50 ± 0.53 and 10.61 ± 1.34, respectively. The CI for the other two agents did not change significantly with time. **Conclusion:** In this rabbit model, ^{99m}Tc-labeled granulocytes, IgG and liposomes all rapidly visualized colonic inflammation. Granulocytes and liposomes showed the highest CI. Technetium-99m-labeled PEG-liposomes may be an attractive alternative for labeled leukocytes to image inflammatory bowel disease, because they can be prepared off the shelf and no handling of blood is required.

Key Words: colitis; liposomes; immunoglobulin; granulocytes; white blood cells; inflammation; inflammatory bowel disease; imaging; technetium-99m

J Nucl Med 1998; 39:2172–2178

Scintigraphic techniques have shown to be useful for evaluating inflammatory bowel disease, providing a rapid and effective method to assess extent and severity of the disease (*1,2*). Several radiopharmaceuticals are available, of which the labeled leukocytes are currently considered to be the most suitable agents (*3–5*). Imaging with ^{111}In-labeled and ^{99m}Tc-hexamethyl propylenamine oxime (HMPAO)-labeled leukocytes have both shown very good correlation with radiology, histology and endoscopy in patients with active inflammatory bowel disease (*1,2*). Compared with ^{111}In, ^{99m}Tc clearly has the advantage of a more favorable radiation dosimetry, better image

Received Jan. 1, 1998; revision accepted Apr. 12, 1998.

For correspondence or reprints contact: Els Th.M. Dams, MD, University Hospital Nijmegen, Department of Nuclear Medicine, P.O. Box 9101, 6500 HB Nijmegen, The Netherlands.